BRIGHAM YOUNG UNIVERSITY

GEOLOGY
S T U D I E S

GEOLOGICAL SOCIETY OF AMERICA

FIELD TRIP GUIDE BOOK

1997 ANNUAL MEETING • SALT LAKE CITY, UTAH

PART 2 TWO

EDITED BY PAUL KARL LINK AND BART J. KOWALLIS

VOLUME 42 • 1997

MESOZOIC TO RECENT GEOLOGY OF UTAH

Edited by
Paul Karl Link and Bart J. Kowallis

BRIGHAM YOUNG UNIVERSITY GEOLOGY STUDIES

Volume 42, Part II, 1997

CONTENTS

A Publication of the
Department of Geology
Brigham Young University
Provo, Utah 84602

Brigham Young University Geology Studies is published by the Department of Geology. This publication consists of graduate student and faculty research within the department as well as papers submitted by outside contributors. Each article submitted is externally reviewed by at least two qualified persons.

Cover photos taken by Paul Karl Link.

Top: Upheaval Dome, southeastern Utah.
Middle: Lake Bonneville shorelines west of Brigham City, Utah.
Bottom: Bryce Canyon National Park, Utah.

ISSN 0068-1016
9-97 700 23870/24290

Preface

Guidebooks have been part of the exploration of the American West since Oregon Trail days. Geologic guidebooks with maps and photographs are an especially graphic tool for school teachers, University classes, and visiting geologists to become familiar with the territory, the geologic issues and the available references.

It was in this spirit that we set out to compile this two-volume set of field trip descriptions for the Annual Meeting of the Geological Society of America in Salt Lake City in October 1997. We were seeking to produce a quality product, with fully peer-reviewed papers, and user-friendly field trip logs. We found we were bucking a tide in our profession which de-emphasizes guidebooks and paper products. If this tide continues we wish to be on record as producing "The Last Best Geologic Guidebook."

We thank all the authors who met our strict deadlines and contributed this outstanding set of papers. We hope this work will stand for years to come as a lasting introduction to the complex geology of the Colorado Plateau, Basin and Range, Wasatch Front, and Snake River Plain in the vicinity of Salt Lake City. Index maps to the field trips contained in each volume are on the back covers.

Part 1 "Proterozoic to Recent Stratigraphy, Tectonics and Volcanology: Utah, Nevada, Southern Idaho and Central Mexico" contains a number of papers of exceptional interest for their geologic synthesis. Part 2 "Mesozoic to Recent Geology of Utah" concentrates on the Colorado Plateau and the Wasatch Front.

Paul Link read all the papers and coordinated the review process. Bart Kowallis copy edited the manuscripts and coordinated the publication via Brigham Young University Geology Studies. We would like to thank all the reviewers, who were generally prompt and helpful in meeting our tight schedule. These included: Lee Allison, Genevieve Atwood, Gary Axen, Jim Beget, Myron Best, David Bice, Phyllis Camilleri, Marjorie Chan, Nick Christie-Blick, Gary Christenson, Dan Chure, Mary Droser, Ernie Duebendorfer, Tony Ekdale, Todd Ehlers, Ben Everitt, Geoff Freethey, Hugh Hurlow, Jim Garrison, Denny Geist, Jeff Geslin, Ron Greeley, Gus Gustason, Bill Hackett, Kimm Harty, Grant Heiken, Lehi Hintze, Peter Huntoon, Peter Isaacson, Jeff Keaton, Keith Ketner, Guy King, Mel Kuntz, Tim Lawton, Spencer Lucas, Lon McCarley, Meghan Miller, Gautam Mitra, Kathy Nichols, Robert Q. Oaks, Susan Olig, Jack Oviatt, Bill Perry, Andy Pulham, Dick Robison, Rube Ross, Rich Schweickert, Peter Sheehan, Norm Silberling, Dick Smith, Barry Solomon, K.O. Stanley, Kevin Stewart, Wanda Taylor, Glenn Thackray and Adolph Yonkee. In addition, we wish to thank all the dedicated workers at Brigham Young University Print Services and in the Department of Geology who contributed many long hours of work to these volumes.

Paul Karl Link and Bart J. Kowallis, Editors

Fault-related Rocks of the Wasatch Normal Fault

JAMES P. EVANS
Department of Geology, Utah State University
4505 University Boulevard, Logan, Utah 84322-4505

W. ADOLPH YONKEE
Department of Geosciences, Weber State University
2507 University Circle, Ogden, Utah 84408-2507

WILLIAM T. PARRY
RONALD L. BRUHN
Department of Geology & Geophysics, University of Utah
717 W.C. Browning Building, Salt Lake City, Utah 84112-1183

ABSTRACT

The Wasatch normal fault is a 370 km long fault zone composed of 10 segments which marks the physiographic boundary between the Basin & Range and Colorado Plateau/Rocky Mountains. Four to eleven km of slip along the Brigham City, Weber, and Salt Lake City segments has resulted in exhumation of numerous fault-related structures which record deformation mechanisms, geochemistry, temperatures, and fluid compositions present during faulting. Deformed Archean rocks at the southern tip of the Brigham City segment (Stop 1) and Oligocene Cottonwood Stock rocks Salt Lake City segment (Stop 4) record an evolution from deep level reaction softening and plastic deformation at $T \simeq 300–350°C$ shallow-level to brittle faulting and cataclasis. Fluid inclusion data from rocks at the southern end of the Salt Lake City segment suggest pore fluid pressure varied from hydrostatic to lithostatic, which suggests Pf may reflect the seismic cycle. The distribution of chlorite-phyllonites and breccias, and subsequent brittle damage zone rocks, indicate the main slip surfaces of the Wasatch fault are enclosed in a weaker, more permeable region of hydrothermally altered and deformed rocks.

The orientation and distribution of structures at the localities also demonstrate the structure of faults at depth near fault bends and segment boundaries. Small fault data at the southern end of the Brigham City segment (Stop 1) are consistent with a S70°W plunging bedrock ridge, with slip complexly distributed across the ridge. Cross faults which intersect the Wasatch fault on the Weber segment (Stop 2) shows on a small scale how slip is distributed in a displacement transfer zone, where non-plane strain exists. The southern tip of the Salt Lake City segment also forms a southwest plunging bedrock ridge where numerous small faults accommodate slip across the segment boundary.

INTRODUCTION

The Wasatch fault zone of northern and central Utah (fig. 1) is one of the most thoroughly studied normal fault zones in the world, both in terms of paleoseismological studies (Schwartz and Coppersmith, 1984; Personius, 1990; Machette et al., 1991, 1992; Machette, 1992; Personius and Scott, 1992; Nelson and Personius, 1993; Hecker, 1993; McCalpin and Nishenko, 1996) and in terms of the characterization of the deformed bedrock in the footwall of the fault (Pack, 1926; Gilbert, 1928; Marsell, 1964, 1969; Parry and Bruhn, 1986, 1987, 1990; Bruhn et al., 1987, 1990, 1992, 1994; Parry et al., 1988; Evans and Langrock, 1994). Numerous field trips along the fault have examined neotectonic features (e.g., Marsell, 1964; Machette, 1988; Nelson, 1988), but few modern field trips have focused on the nature of bedrock deformation and its use in interpreting the processes active along the fault. This field trip will visit localities along the Wasatch fault where detailed field mapping, structural petrography, geochemistry, geochronology, and modelling have focused on the style and distribution of

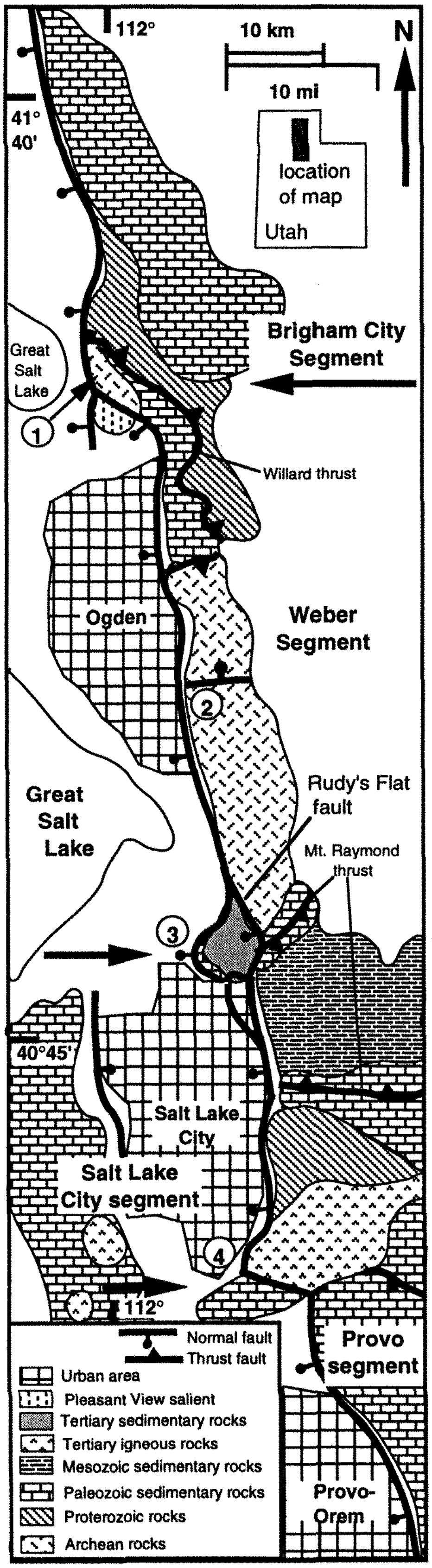

deformation adjacent to the fault, and where inferences regarding fluid flow and mechanical properties adjacent to the fault can be made.

GEOLOGIC SETTING

The Wasatch fault has long been recognized as a major fault which marks the eastern physiographic limit of the Basin and Range Province (Gilbert, 1890, 1928; Eardley, 1939). The fault is approximately 370 km long, and consists of 10 fault segments which extend from southern Idaho to central Utah (Gilbert, 1928; Swan et al., 1980; Machette et al., 1991, 1992). The segments are defined by Holocene slip histories as determined from trenching studies and on the basis of detailed mapping along the fault zone. Prominent topographic salients, where the mountains protrude westward and are underlain by bedrock, coincide with many of the segment boundaries (Machette et al., 1992; Wheeler and Krystinik, 1992). Gilbert (1928) was apparently the first to recognize and describe the salients that mark the boundaries between the Brigham City, Weber, Salt Lake City, and Provo segments (fig. 1), which are the focus of the stops described in this field guide. These bedrock salients may be rupture barriers between segments for long periods of time (Wheeler and Krystinik, 1992; Cowie and Scholz, 1992) and thus record deformation over a large time span of the fault.

The fault cuts a wide variety of rock types and structures along its entire trace (Eardley, 1944; Baker, 1964; Crittenden, 1965a, b; Hintze, 1980; Crittenden and Sorensen, 1985a, b; Bryant, 1990; Personius, 1990; Personius and Scott, 1992; Machette, 1992; Nelson and Personius, 1993). The Wasatch fault is superimposed on complex Cretaceous thrusts and folds of the Sevier fold and thrust belt (Eardley, 1944; Crittenden, 1974; Royse et al., 1975; Zoback, 1983; Smith and Bruhn, 1984; Yonkee et al., 1992; Arabasz et al., 1992). The major thrust structures are, from south to north, the Charleston-Mt. Nebo, Absaroska, and Willard thrusts and the imbricate stack of thrusts in the Ogden duplex (Schirmer, 1988; Yonkee, 1992). These thrust sheets have been cut by the Wasatch fault, exposing Late Archean through Jurassic rocks in the footwall.

Motion on the Wasatch fault zone may have started as early as 17.6 ± 0.7 U.C. Ma, based on a K-Ar date on hydrothermal sericite on rocks at the southern tip of the

Figure 1. Generalized geologic map of the Wasatch Front. Numbers indicate stops for this trip. The large arrows indicate the location of segment boundaries. Geology from Davis (1983, 1985), Personius (1990); Nelson and Personius (1993), Bryant (1990), and Personius and Scott (1993).

Salt Lake City segment where the fault cuts the Cottonwood stock (Parry et al., 1988). Apatite fission track ages of 9.6 to 8.2 my (Parry et al., 1988), and apatite fission track uplift rates of 0.4 mm/year for the past 10 million years (Naeser et al., 1983), suggest that rapid uplift along the central Wasatch fault began about 10 million years ago. Bryant et al., (1989) show that sedimentation rates in basins west of the Wasatch fault increased significantly at 10–12 million years ago, suggesting the onset of rapid slip along normal faults in the area began at that time.

Geophysical characterization of the region (Zoback, 1983; Mabey, 1992) shows that the basins in the hanging walls of the fault segments vary in thickness, and that numerous geophysical anomalies trend at high angles to the segments at or near segment boundaries. Gravity modelling suggests basin fill sequences are 1.2 to 3.8 km thick. Basin form is variable, with inferred maximum thicknesses of basin-fill roughly correlative with the centers of segments (Zoback, 1983; Mabey, 1992).

Historical seismicity in the area has been characterized by small to moderate events scattered throughout the hanging wall and footwall of the fault (Zoback, 1983; Arabasz and Julander, 1986; Arabasz et al., 1978, 1992). Locations of earthquakes in the area tend to be clustered at the northern and southern ends of the entire fault zone (Arabasz et al., 1992, their fig. 17; Pechman, 1992) with noteable gaps on the Weber and Salt Lake City segments. Earthquakes on or near the Wasatch fault have been small, whereas the paleoseismologic data show that the fault segments are capable of M 7–7.5 earthquakes (see Machette et al., 1992 for a complete discussion of paleoseismological analyses of the Wasatch fault).

On this trip, we will travel to exposures of bedrock in the footwall of the Wasatch normal fault and examine evidence for deformation and fluid-rock interactions along the fault. These exposures reflect deformation at greenschist grade to shallow levels, and may record deformation for most of the fault history. We will first travel north to the bedrock salient known as the Pleasant View salient (stop 1), where Archean-Early Proterozoic rocks are in the footwall of the Wasatch normal fault. We then examine structures near Ogden in Paleozoic rocks (stop 2), shallow level deformation at the Beck Street Spur (Stop 3), and conclude with an examination of deformation of the Oligocene Little Cottonwood stock (stop 4).

Road Log

0.0		Depart the Salt Palace. Drive south on West Temple. Turn west on 1st South.
0.3	0.3	Turn right (north) on 2nd West.
2.7	3.0	Monroc Sand and Gravel quarries. The road veers around the western end of the Beck Street salient at the northern end of the Salt Lake City. We will return to this site for Stop 3.
1.0	4.0	Merge with I-15.
4.8	8.8	View to east of basement rocks of Late Archean-Early Proterozoic Farmington Canyon Complex (Eardley and Hatch, 1940; Bryant, 1984, 1988) which lie on the steeply dipping eastern limb of a basement-cored anticline. "B" on hill slope to the east is at the Bonneville level of Lake Bonneville. Antelope Island visible to the northwest consists of Precambrian basement and gently dipping sedimentary cover rocks that lie on the western limb of a basement-cored anticline (Yonkee, 1992).
5.1	13.9	Quaternary landslide complex is visible to east.
2.0	15.9	Junction with U.S. Highway 89. Continue heading north on I-15.
1.0	16.9	Bumpy terrain in golf course to east is part of a lateral spread deposit that may have formed by ground failure during past earthquakes (Pashley and Wiggins, 1972).
4.0	20.9	View of Antelope Island to west.
4.5	25.4	The highway passes along the western (distal) edge of the Weber delta which was built out into ancient Lake Bonneville.
7.3	32.7	Descend onto alluvial deposits of Weber River.
3.9	36.6	View to the east shows the Willard and Ogden thrust systems, which display complex lateral ramps and branching of thrusts in the Wasatch Range. Details of this region are presented in Link et al., (1985, 1990; and Yonkee, 1992; Yonkee et al., this volume).

We are in the hanging wall of the Weber segment of the Wasatch normal fault, which last ruptured about 0.5 ka (Machette et al., 1989, 1992). Net displacement across the Wasatch fault zone in the Ogden area probably exceeds 5 km, and a deep hanging wall basin is filled with Miocene and younger deposits underlies the area to the west.

A view to the northeast from here shows the prominent shorelines of the Provo and Bonneville levels of Lake Bonneville, which are cut by younger alluvial fan and debris flow deposits sourced in the steep canyons beneath Ben Lomond Peak.

9.8 46.4 Exit 354. Take the exit and continue north on US 89.

1.5 47.9 Turn right onto the gravel road to the gravel pit owned by Jack B. Parsons Co. Note: This is a private road.

0.75 48.6 Turn left onto the road which is parallel to a canal. We are traversing the Pleasant View salient, which Gilbert (1928) first recognized as a bedrock-cored horse, mantled by deposits of Lake Bonneville.

1.1 49.7 Cross an outwash channel on the alluvial fan emanating from Pearson's Canyon. These debris flow channels were active in 1983 and 1984, and coarse material deposited during this event is on both sides of the road. Pearson's Canyon is at the 40° bend in the Wasatch fault (figs. 2, 3), which lies at the western margin of the bedrock to the east (Personius, 1990; Crittenden and Sorensen, 1985a). The scarp height south of Pearson's Canyon is 32 m, with an estimated offset of an alluvial fan surface of 19 m (Personius, 1990).

0.8 50.5 A concrete bridge crosses the canal. Turn onto the bridge, and follow the dirt track to the end (approximately 0.2 miles). Park.

Stop 1. We are on the apex of the Holmes Canyon alluvial fan, which is an active region of coarse debris deposition (figs. 2, 3). Personius (1990) shows a scarp height of 22 m, and an offset of 18.5 m on the top of the alluvial fan surface here. Immediately to the east are exposures of deformed bedrock adjacent to the Wasatch fault.

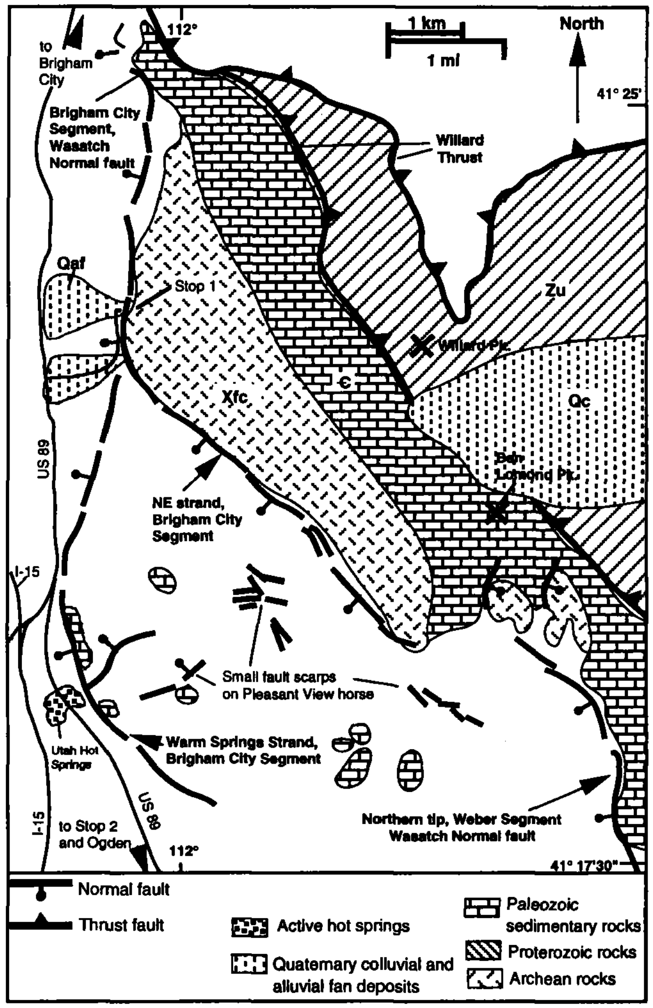

Figure 2. Detailed map of the southern termination of the Brigham City segment of the Wasatch Fault Zone. Bold lines indicate fault traces. The salient is formed by a left step between the Brigham City and Weber segments, and a western fault strand which bounds the Pleasant View horse. XFC–Farmington Canyon Complex; –Cambrian rocks; Zu–undifferentiated Proterozoic rocks in the hanging wall of the Willard thrust; Qc–Colluvium; Qaf–Alluvial fans. Unshaded region west of the Wasatch Fault is Lake Bonneville sediments. Geology from Crittenden and Sorenson (1985a, b); Personius (1990).

We will examine fault-related rocks at the southern end of the Brigham City segment, in the Pleasant view salient. The Brigham City segment has a surface trace length of 40 km (Personius, 1990) and trends roughly north-south, except at the southern end of the segment, where it bends sharply to a N40°W trend (fig. 2) (Personius, 1990). The southern tip of the Brigham City segment overlaps the northern Weber segment by approximately 1.5 km at a 1 km left step here (Machette et al., 1991, 1992).

The Farmington Canyon Complex comprises the crystalline "basement" for the northern part of the Wasatch fault (Bryant, 1988), and is exposed in the footwall throughout the southern third of the Brigham City segment (fig. 2; Crittenden and Sorensen, 1985a,b; Personius, 1990). Rocks of the Farmington Canyon Complex are equigranular quartz-feldspar-biotite-hornblende gneiss. Foliation is defined by 1–10 cm mineral banding, and aligned micas and hornblende grains. Hanging-wall units of the Brigham City segment consist of Quaternary lacustrine sediments along the north-trending part of the segment (Personius, 1990) and a horse of Cambrian sedimentary rocks of the Pleasant View salient (Gilbert, 1928; Crittenden and Sorensen, 1985b).

The horse is bounded on the northeast by the northwest-striking strand of the Brigham City segment. On its west

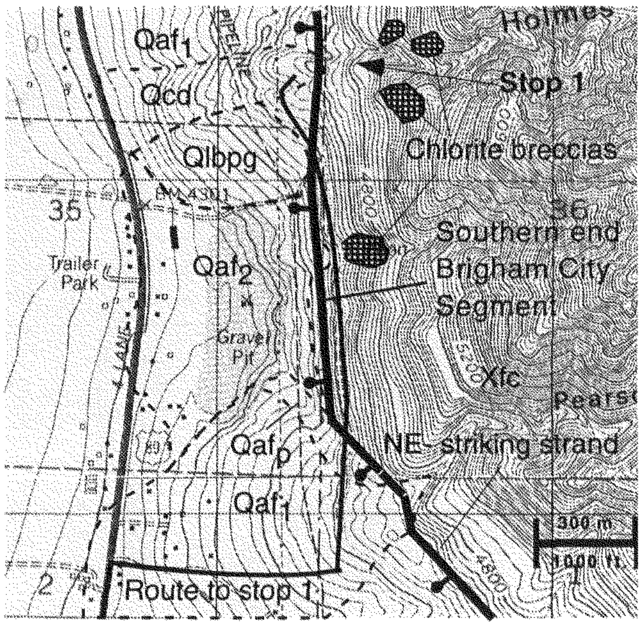

Figure 3. Detailed map of stop 1 geology. The fault trace corresponds closely with the Provo shoreline. At the mouth of Holmes Canyon, an alluvial fan is out by a scarp 22 m high, and an offset of 18 m. Chlorite breccias are indicated. Key to deposits on the hanging wall: Qafp–alluvial fan from Provo-level time (ca 1–3 14000 yrs b.p.); Qaf_1, Qaf_2-alluvial fans younger than Provo-level; Olbpg–lacustrine near-shore grand deposits; Qcd–Debris flow deposits. Base map from Willard, Utah 7.5 minute quadrangle; geology from Personius, 1990; Evans and Langrock, 1994.

side the horse is bounded by an inferred southward continuation of the north-trending part of the Brigham City segment, termed the Hot Springs strand (fig. 2) (Gilbert, 1928; Crittenden and Sorensen, 1985b; Personius, 1990). Dip-slip displacement on the NW strand of the Brigham City segment is ~1.7 km, based on reconstruction of footwall and hanging-wall strata (Crittenden and Sorensen, 1985b). NE- and NW-striking Quaternary fault scarps cut the horse, and are especially numerous near the southern tip of the Brigham City segment (Personius, 1990).

Based on cross-cutting relationships, mesoscopic structures, and microstructures, we (Evans and Langrock, 1994) identify three major types of fault-related rocks and mesoscopic faults developed in the Farmington Canyon Complex adjacent to the Wasatch fault zone, and these faults are the focus of this stop. From oldest to youngest, these fault-related rocks are: (1) green and brown chlorite breccias and phyllonites, (2) planar, fretted "purple and brown weathered" fault surfaces, and (3) maroon and purple, highly polished, planar striated fault surfaces.

1. Chlorite breccias and phyllonites form an irregularly shaped, narrow north-trending band in the footwall of the north-trending part of the Brigham City segment (fig. 3). Phyllonites are characterized by millimeter to centimeter thick, 20°–40° west-dipping foliation defined by chlorite-quartz layers (fig. 4). Down-to-the west motion is indicated by locally developed S-C fabrics developed at outcrop and thin-section scales (fig. 5a). Chlorite breccias consist of random-fabric zones which dip 30°–50° west in the immediate footwall of the Brigham City segment. The chlorite breccias comprise the majority of the chlorite zones.

   Microstructures in the phyllonites consist of dynamically recrystallized quartz which forms elongated bands parallel to foliation (fig. 5a), and muscovite-chlorite which exhibit interlayer kinking and basal slip. Few feldspar grains remain in the phyllonite, and altered feldspars lie at the edges of the phyllonites.

   The shallow dip of foliation of the phyllonites and their similarity to phyllonites and chlorite breccias in the footwall of the Salt Lake City segment (Bruhn et al., 1987; Parry and Bruhn, 1986; Stop 4 of this trip) is consistent with these rocks representing Wasatch fault-related rocks that formed at depth and have been uplifted in the footwall. However, unlike the fault-related rocks developed in Eocene-Oligocene quartz monzonites on the Salt Lake City segment (Bruhn et al., 1987), Farmington Canyon Complex rocks may also record Sevier contractional deformation (Yonkee, 1992).

2. Brown and purple fault surfaces are characterized by crescent-shaped, strike-parallel fractures, pits, and pockmarks that cut phyllonites, chlorite breccias, and the otherwise undeformed Farmington Canyon Complex protolith gneiss. Fretted, purple and brown weathered faults are planar to slightly curved, and the zone of deformation associated with a single surface is 1–10 cm thick. The fretwork faults are found in a broad zone adjacent to the north and NW-trending parts of the Wasatch fault, and their density appears to decrease east and northeast away from the trace of the Wasatch fault. Slickenlines are rare and tool marks and grooves are uncommon on these faults. Strike-parallel fractures inclined by 20°–40° to the fault surfaces resemble tensile or crescent fractures (Petit, 1987), which indicate down-to-the west motion.

   Microstructures of the fretted purple weathered faults record fracture, frictional slip, and cataclasis (fig. 5b). Iron-oxide mineralization commonly fills fractures and thin cataclasite zones, suggesting at least limited fluid flow during development of these faults. Zones of distributed cataclasis are up to 10

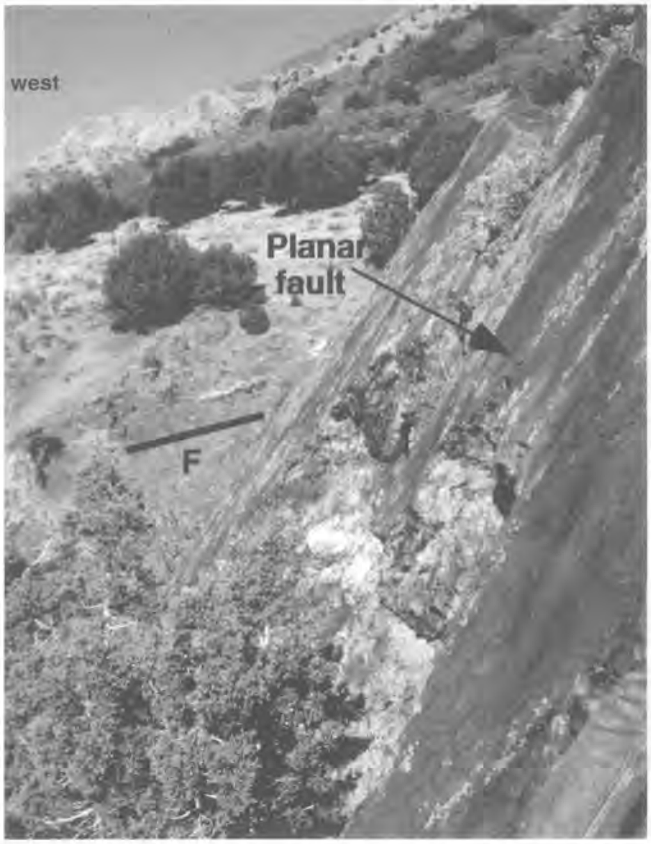

Figure 4. Outcrop photo of a younger, purple-weathered, planar fault surface in foreground dipping approximately 55° west, with 20° west-dipping chlorite phyllonites in the background (line S indicates dip of foliation). Trace of Wasatch fault is approximately 15 m to the west (left) of this view. View is to the north, from south-side of Holmes Canyon at stop 1. Wasatch Range is in the background.

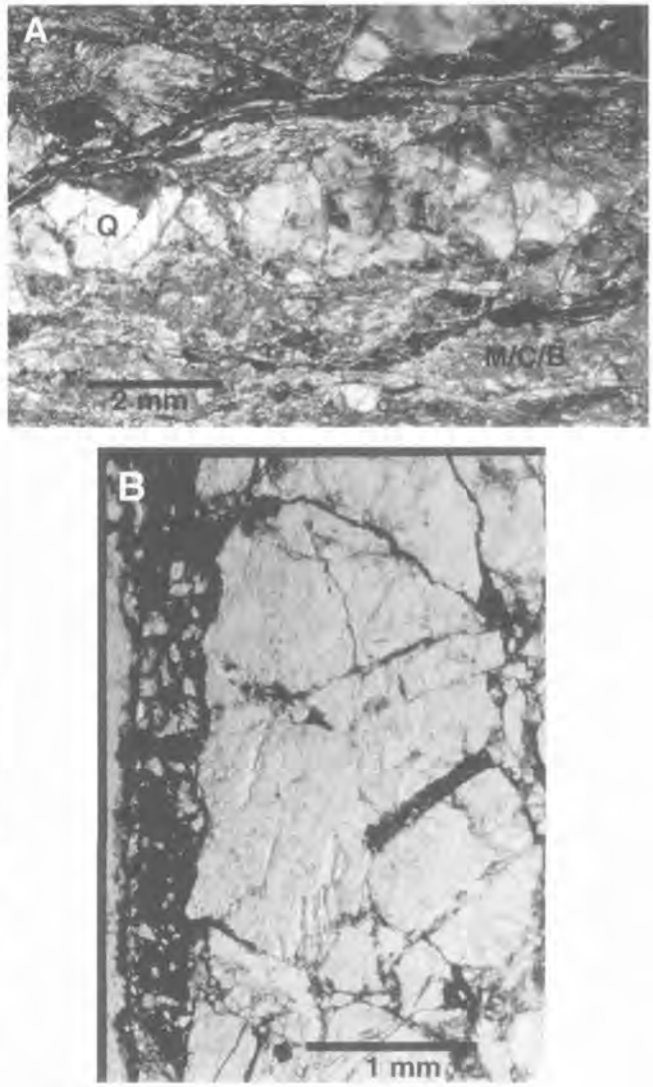

Figure 5. Photomicrographs of thin sections of samples at stop 1.
A. Plastically deformed chlorite-muscovite phyllonite with west-dipping foliation developed in the footwall of the Wasatch fault at stop 1. Q–fractured quartz grain with some plastic deformation evident; M/C/B–Muxorite-Chlorite-Biotite. Cross-polarized light view.
B. Plane-polarized light view of the narrow, highly polished faults superposed on fretted fault network. The narrow polished fault zone is approximately 0.2 mm wide at left side of photo, and consists of very fine grained hematite (crystallinity determined by x-ray diffraction). The network of fractures are due to brittle deformation related to the fretted faults, and consists of intergranular fractures filled with hematite and microcataclasite.

cm thick, and the fault-related rocks are all random-fabric cataclasites.

3. The most striking mesoscopic faults at Stop 1 are west-dipping, maroon and purple, highly polished, planar faults. These faults are distributed throughout the study area, cut the phyllonites, chlorite breccias, and fretted faults, and their density decreases away from the trace of the Wasatch fault. The highly polished surfaces commonly have tool marks and grooves, some of which are curved, which record asperity ploughing and slip of the hanging wall in a down-to-the west sense. The fault surfaces are commonly only several millimeters thick.

Microstructures of the highly polished surfaces and related rocks indicate purely brittle deformation. Rocks adjacent to the narrow slip surfaces exhibit intra- and intergranular fracture, and very narrow zones of cataclasis (fig. 5b). The narrow slip horizons consist of very fine-grained hematite, usually in sharp contact with adjacent cataclastically deformed gneiss. Scant evidence from loose float blocks, and from several in-place hematite veins suggests these faults may have first initiated as hematite-filled veins or coated fractures, and evolved into polished, planar surfaces.

The extreme polish of the mineralized surfaces and the microstructures may indicate extremely fast rates of slip on these surfaces (Grocott, 1981), which could represent seismic slip at several km depth, where confining pressures were large enough to maintain surface contact during a slip event. Conversely, these highly polished surfaces may represent aseismic creep (Power and Tullis, 1992), making a unique interpretation of slip rate for the highly polished surfaces difficult.

The orientations, spatial distributions, and characteristics of the three fault types represent an evolution from deep-level reaction softening and plastic deformation exhibited in the phyllonites and chlorite breccias to zones of cataclasite represented by the fretted purple-weathered faults and the polished planar faults. Phyllonites and chlorite breccias are restricted to the north-trending part of the Brigham City segment, which suggests deeper levels of the fault zone were exhumed there, or that more recent slip has stepped into the footwall on the northwest-striking strand, cutting out fault rocks from deeper levels.

Kinematic analyses of small fault populations in the footwall of the Brigham City segment constrain the orientations and relative magnitudes of principal stresses, and help examine the geometry of deformation in the footwall. We examined (Evans and Langrock, 1994) fault slip data for dominant clusters in slip directions and fault orientations and mean fault plane solutions, and inverted the fault data for principal stress orientations using the method of Gephart (1990a,b). Orientations of small faults on standard lower hemisphere stereograms (fig. 6) and kinematic analysis provide a first-order estimate of the orientation best-fit fault planes and a fast estimate of the orientations of the maximum and minimum principal stresses using the seismological convention for P and T axes. The stereograms and fault kinematic analyses show that along the north-striking trace, strikes of small faults roughly parallel the strike of the Wasatch fault zone.

In the corner region and along the northern part of the northwest-striking strand of the Brigham City segment, the small faults strike northwest or northeast and slickenlines indicate slip occurred down-to the WNW, WSW, or south. Small oblique-slip components of both senses exist for most of the faults. The fault plane and slickenline data indicate oblique-slip motion generally on two sets of faults and non-plane strain behavior of these portions of the fault whereas the pseudo-nodal plane solutions yield nearly pure normal slip. The mean slip vectors along the NW-striking strand form a crude N70°W striking girdle distribution. This suggests that while fault slip occurred along faults of several orientations, including some at high angles to the main trace of the fault, slip was restricted to a NW-striking band of deformation.

The kinematic and stress inversion analyses of the small faults, along with the mapping of the hanging wall horse (Personius, 1990) indicate that the segment boundary zone is a broad region of complex footwall and hanging-wall deformation. The different orientations of faults and slip vectors in the footwall, as well as the multiple orientations of faults in the Pleasant View horse (fig. 2) (Personius, 1990), may represent changes in the orientations of principal stresses over space or time, or represent non-plane strain behavior at the end of the fault segment (Scholz, 1990; Cowie and Scholz, 1992).

If the zone of deformation we observe is the result of fault tip damage, we would expect to see a similar, older damaged zone in the footwall to the north. The absence of a knot of complex faulting adjacent to the north-striking segment may be explained by several hypotheses: a) The damaged zone near the fault tip there may have been smaller, and was obliterated by later faulting, b) much of the damage occurred in the hanging wall, c) little damage occurred ahead of the relatively "cleanly" propagating shorter, north-striking fault segment, whereas the present Brigham City segment has developed a broad damaged zone at the fault tip due to encountering a structural complexity, or d) stresses on the fault changed over time.

2.9	53.4	Return to Highway 89 driving southward, the canal and returning through the gravel pit. Drive south on Highway 89 toward Ogden.
1.6	55.0	The road skirts Cambrian Tintic quartzites to the east, and hot springs emanating from the Wasatch fault to the west.
7.8	61.2	Highway 89 intersects with Washington Blvd in Ogden. Merge south. The rocks in the mountains to the east consist of thrusted Archean-Early Proterozoic basement and Cambrian strata in the Ogden Duplex (Schirmer, 1988; Yonkee, 1992).
1.0	62.2	Intersection with 12th South (Highway 39). Turn left (east).
1.2	63.4	Intersection with Harrison Blvd. turn right (south). We are driving up to the Provo-level delta of Lake Bonneville.
1.0	64.4	Intersection with 2100 South. Turn left (east).
1.0	65.4	Drive east to the trail head at the end of the street (fig. 7).
Stop 2.		Stop 2 is located along the Weber segment near a small fault bend that was first described by Gilbert (1928). This area contains a northern fault and southern

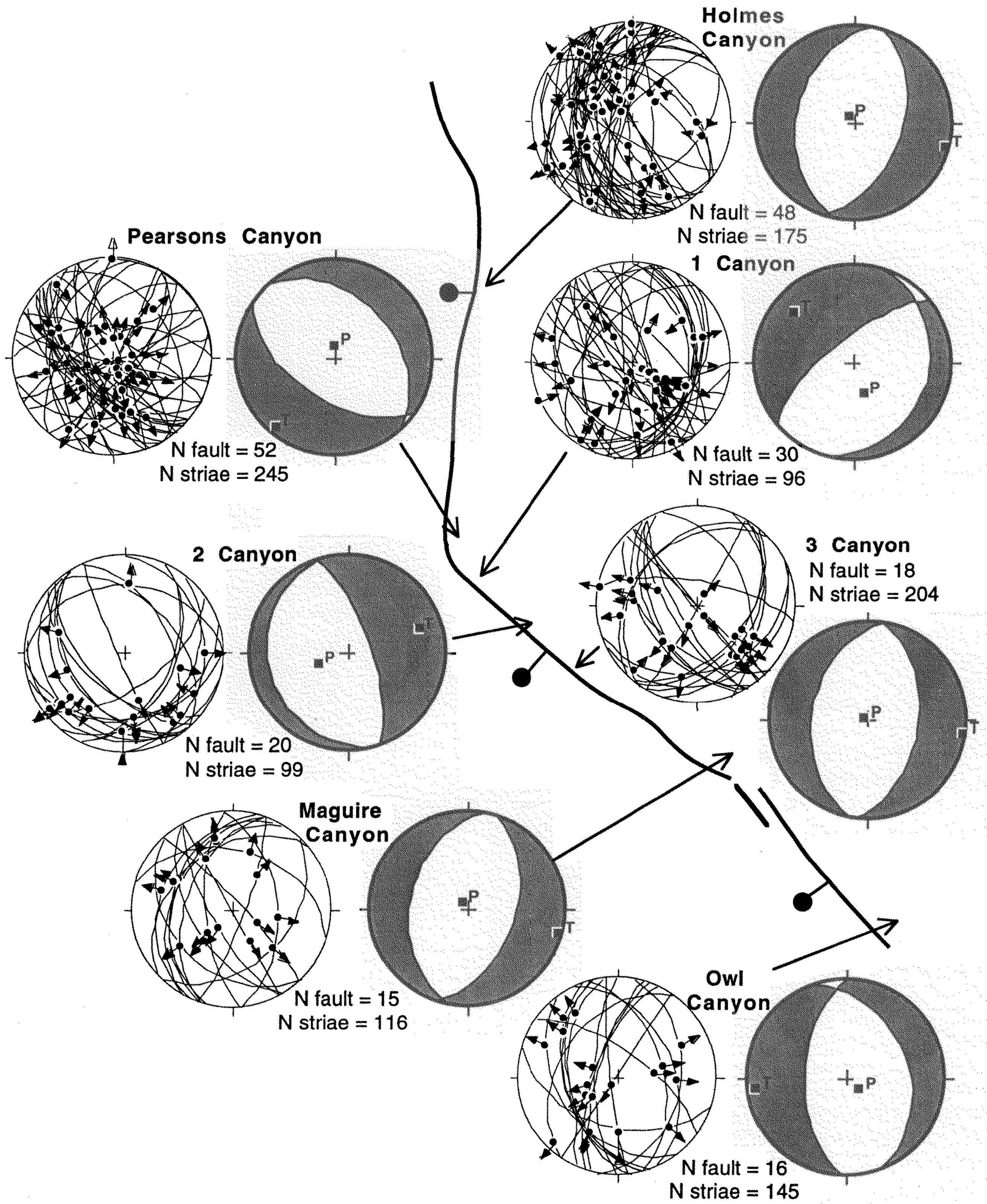
Holmes Canyon
N fault = 48
N striae = 175
Pearsons Canyon
N fault = 52
N striae = 245
1 Canyon
N fault = 30
N striae = 96
2 Canyon
N fault = 20
N striae = 99
3 Canyon
N fault = 18
N striae = 204
Maguire Canyon
N fault = 15
N striae = 116
Owl Canyon
N fault = 16
N striae = 145

fault that both place Cambrian Tintic Quart- zite against Quaternary unconsolidated deposits, and an east-striking cross fault that connects the two main faults, forming a composite cross-fault-intersection structure (fig. 7). The northern, southern, and cross faults are divided into approximately planar sections, but in detail, sections display roughness at a range of smaller scales, including crude ridges and troughs subparallel to slip directions. Sections of the northern fault dip 40 to 50° west and have west- to southwest-trending slip lineations. Sections of the southern fault also dip moderately westward and have west- to southwest-trending slip lineations. The cross fault dips steeply south, connects the northern and southern faults, which displays a 100 m left step along the cross fault. The cross fault and associated secondary faults have varying combinations of normal and sinistral slip, and displacement decreases to the east where the cross fault (C) continues into the footwall of the main faults. The northern fault (N) forms a bend along the intersection with the cross fault, and a fault-bounded bedrock wedge (S) is developed where the southern fault branches near the cross-fault intersection (fig. 7). Sections around the northern bend define an approximately cylindrical geometry of the fault, and slip directions diverge slightly around the bend. The change in slip directions, development of complex secondary faults near the cross fault, and formation of the bedrock wedge probably record displacement transfer and non-plane strain in the region connecting the northern and southern faults.

Figure 6. Lower hemisphere equal-area plots which depict the orientations of fault planes and slickenlines at seven localities along the Brigham City-Weber segment boundary zone. Kinematic solutions of the data give orientations of the nodal planes and mean compressional (P) axes and extensional (T) axes. Numbers indicate groups of data referred to in text. Open symbols indicate mean slip vectors.

Small faults across the bend can be interpreted to be due to east-west extension despite the variable slip vector orientations. From Evans and Langrock (1994).

Although some differences exist, the geometry and kinematics of this small-scale structure are similar to those in the boundary between the Salt Lake City and Provo segments (see stop 4), indicating that cross-fault-intersection structures may be important at a variety of scales. East-striking cross faults of varying trace length and displacement are widespread along parts of the Wasatch fault (fig. 1). Timing of slip on these faults is uncertain; some may have initiated during Mesozoic thrusting and been reactivated during Cenozoic extension, and others may be directly related to Cenozoic extension. Here the cross fault probably overlapped with early development of the northern and southern faults that cut bedrock, but these faults have not been active during the Holocene when near-surface faulting in the Wasatch fault zone shifted westward within surficial deposits. Some intersections with larger cross faults may develop into rupture boundaries (as between the Salt Lake City and Provo segments, stop 4), depending partly on the scaling and geometric relations between faults. Some intersections may affect, but not stop, rupture propagation, and some intersections may have no significant affect on ruptures. Both situations probably occurred here during recent episodes of faulting.

1.0	66.4	Return to Harrison Blvd. Turn right (south). As we drive south, we traverse the top of the Provo-level delta. The surface trace of the Wasatch fault in this area is marked by a single scarp 10–34 m high (Nelson and Personius, 1993).
2.6	69.0	Pashley & Wiggins (1972) and Nelson & Personius (1993) interpret the hummocky terrain on the left to mark a sequence of lateral spread and landslide deposits.
1.7	70.7	Road merges with Highway 89. Turn left (east). We descend to the Weber River flood plain.
13.4	84.1	Highway 89 merges with I-15 south bound. The surface trace of the Wasatch fault along this stretch splits into 2 or 3 scarps. Approximately 4.3 miles north of I-15 lies the site of the Kaysville trench, one of the first paleoseismology trenches in the Great Basin (Swan et al., 1980;

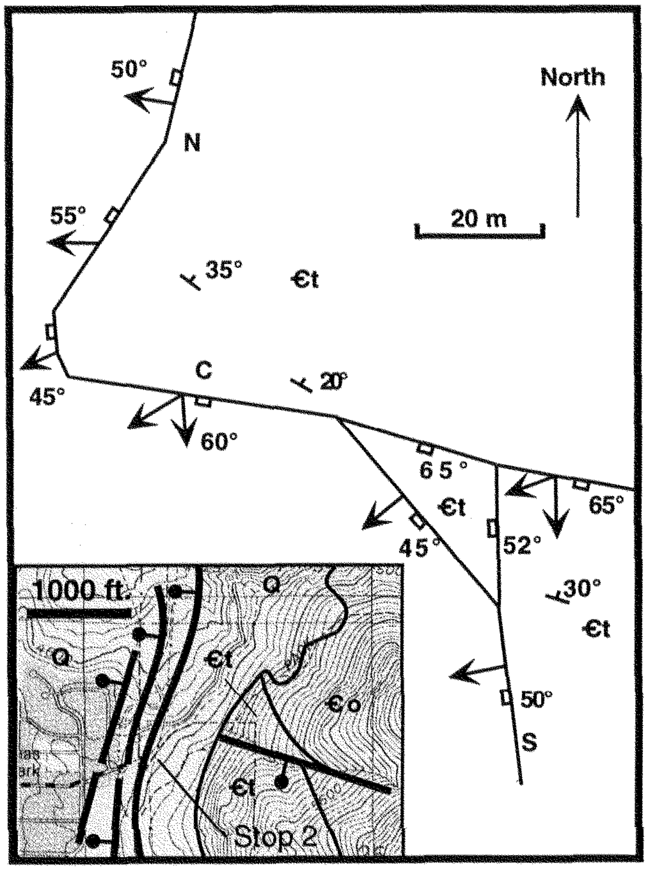

Figure 7. Generalized geologic map of composite cross-fault intersection structure at Stop 2, Ogden, Utah. Strike and dip of approximately planar fault sections and average slip directions are indicated. Units are: Ct–Cambrian Tintic Quartzite; Co–Cambrian Ophir Formation; and Q–Quarternary lacustrine, colluvial, and alluvial fan deposits. Dashed line indicates field trip route.

McCalpin & Nishenko, 1996). The last rupture on this segment was approximately 900 years ago, and 5 events dating back to 6400 years b.p. are recorded on the Weber segment (McCalpin & Nishenko, 1996).

1.0	95.1	Highway 89 exit. Get off I-15.
2.7	97.8	Continue south on Highway 89 past the Monroc Gravel Plant, and pull off in the industrial area on east side of street. Stop 3.

Stop 3. Tectonics of the Warm Springs fault zone and Salt Lake City segment of the Wasatch fault zone. Stop at pull out approximately 0.5 miles south of MONROC headquarters.

The Salt Lake City segment of the Wasatch fault zone is about 35 km long and consists of several approximately planar sections, each 3 to 12 km in length, that meet along fault bends and branches (fig. 1; Bruhn et al., 1987; Personius and Scott, 1992). Estimated dips range from 30 to 60°. Paleostress analyses along the Salt Lake City segment have indicated a subhorizontal minimum compressive stress trending between 230 and 250°, consistent with west to southwest-trending normal to oblique slip along the fault sections (Bruhn et al., 1987; Yonkee and Bruhn, unpublished data).

The Salt Lake City salient, a complexly faulted and partly buried west-southwest-trending ridge of Tertiary and Paleozoic bedrock (Van Horn, 1982; Van Horn and Crittenden, 1987), forms the northern boundary of the Salt Lake City segment. Gravity and drill hole data indicate that the bedrock ridge continues westward into the Salt Lake Valley (Zoback, 1983), and a diffuse belt of epicenters of small earthquakes lies above this ridge. The Salt Lake City salient is a non-conservative barrier that separates the Weber and Salt Lake City segments (Schwartz and Coppersmith, 1984; Machette et al., 1991). The salient is largely covered by gently east-dipping Tertiary clastic and volcaniclastic deposits and these deposits are separated from Precambrian bedrock and steeply dipping Paleozoic rocks by the Rudys Flat fault along the eastern boundary of the salient. This west-dipping normal fault is "scoop-shaped" and varies in strike from northwest to northeast. The interior of the salient contains several north- to northwest-striking synthetic and antithetic normal faults, and several northeast-striking faults. The salient is partly bounded on the south by the west-northwest-striking Virginia Street fault. The north-striking Warm Springs fault separates Paleozoic and Tertiary bedrock from Quaternary deposits along the western margin of the salient (fig. 8) (Gilbert, 1928; Marsell, 1964, 1969; Scott, 1988). This fault appears to bend around the salient and a northeast-striking branch bounds the northwestern margin of the salient. A possible fault branch also continues north of the salient (Van Horn, 1982). The southern extent of the Warm Springs fault is uncertain, and this fault may be en echelon or merge with the main part of the Salt Lake City segment.

The Warm Springs fault dips 40 to 80° west within the MONROC quarries, and places southeast-dipping beds of Mississippian limestone in the footwall against Quaternary deposits in the hanging wall (fig. 8) (Marsell, 1969; Paulis and Smith, 1980). Deposits of Lake Bonneville are offset by 10 to 15 m across the fault, probably recording multiple slip events (Gilbert, 1928; Marsell, 1964). Fault surfaces display two dominant sets of slickenlines, a west-southwest-trending set and an older west-northwest-trending set (Pavlis and Smith, 1980). Fault surfaces also display undulations

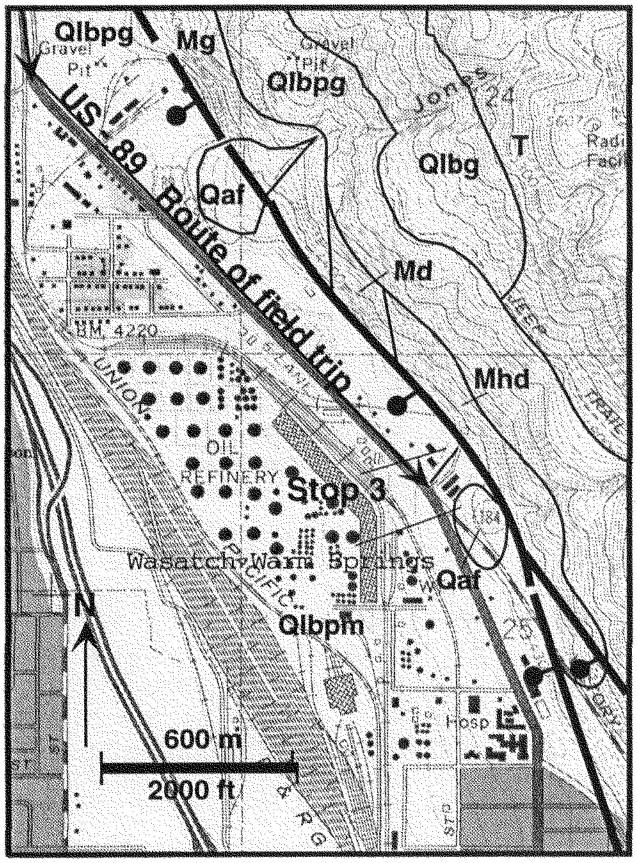

Figure 8. Geologic map of the Warm Springs section of the Wasatch fault at stop 3. Paleozoic carbonates are in the footwall here, and are overlain by Tertiary sediments and Lake Bonneville deposits. Mg–Gardison Formation; Md–Deseret Limestone; Mhd–Hamburg/Dunct Formations; T–Tertiary sediments; Qlbpg–lacustrine gravels of undifferentiated lake cycles; Qlbg–Bonneville-stage lacustrine gravels; Qlbpm–Fine-grained lacustrine sediments; Qaf–alluvial fan deposits.

with wavelengths and amplitudes of millimeters to meters. Most undulations are aligned subparallel to slickenlines which are oriented approximately down the dip of the fault.

Pavlis and Smith (1980) show that slickenline data reflect dip slip displacement, with 3 or 4 events recorded by tool marks on the limestones. Photomicrographs of the fine-grained carbonate that forms a carapace have cataclastically deformed limestone grains entrained in the carbonate (fig. 9). The carbonate has a crude layering in thin section and outcrop. Ridges with crests parallel to dip and faint strike suggest the carbonate was explaced during faulting.

1.4 99.2 Drive south on Highway 89 to 5th North. Turn right (west). Proceed 0.5 miles to I-15, and return to I-15 south bound. As we travel southward along the Salt Lake Valley, views of the geology of the Wasatch Range to the east are clear. The Wasatch Range east of the University of Utah (look for the U on the mountain front) to several miles south of Parleys Canyon consists of northeast trending folds in Triassic and Jurassic strata (Crittenden, 1965b; Van Horn and Crittenden, 1987; Bryant, 1990). These folds lie in the hanging wall of the east-striking, north-dipping Mt. Raymond thrust which intersects the mountain front due east of exit 304. South of the thrust, Cambrian and Proterozoic sedimentary rocks can be seen along the mountain front. At exit 298, we are due east of Little Cottonwood Canyon, which roughly coincides with the northern boundary of the Eocene Little Cottonwood Stock. Little Cottonwood Canyon was glaciated during the Pleistocene, and lateral moraines at the mouth of the Canyon are cut by the Wasatch fault, forming spectacular fault scarps depicted in many texts.

17 116.2 Exit 297 for Highway 71 (12,300 South). Get off I-15 and head east on Highway 71.

1.1 117.3 Turn right on 700 East. Drive 1 block, and turn east on the continuation of 12300 South (fig. 10).

1.9 119.2 Paved road ends. Turn right onto the gravel road.

0.8 120.0 Pull off road and park. Stop 4: Cherry Creek Canyon (fig. 10).

Stop 4. Boundary between the Salt Lake City and Provo segments. Park along the side of the gravel road. Discussion of large-scale kinematics and short hike to observe nature of fault zone. Four features in this area are noteworthy: (1) kinematics of fault segments in the boundary are important in controlling rupture nucleation and propagation; (2) deeper levels of the fault zone were complex, up to several hundred meters wide, and consisted of anastomosing minor faults; (3) hydrothermal alteration and fluid-pressure fluctuations were important in evolution of the fault zone; and (4) the intensity and nature of alteration and fracturing produced changes in physical properties of the fault zone.

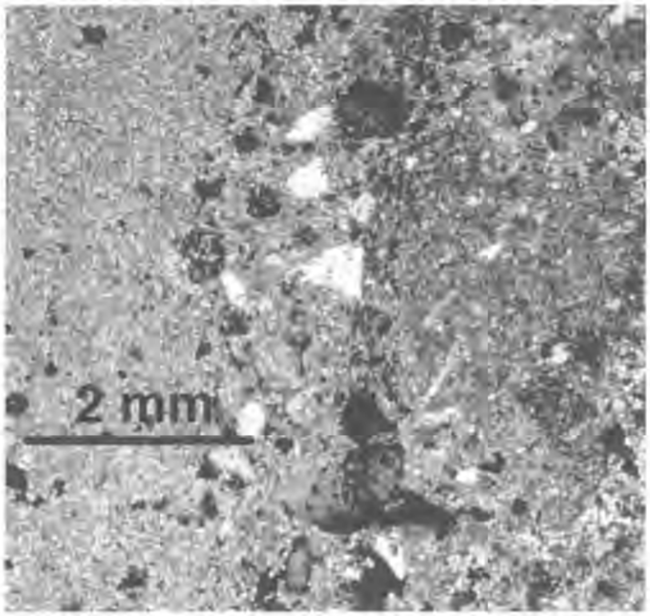

Figure 9. Cross-polarized light photomicrograph of the carbonate carapace formed along the Warm Springs portion of the Wasatch fault at stop 3, Beck Street locality. Before recent excavations the 1–4 cm thick, spelian calcite, was distributed across a large portion of the fault surface, and exhibited elongation undulations which have long axes oriented down-dip, and have faint down-dip lineations. This thin section exhibits a foliation parallel to the fault (vertical in this view). Small angular carbonate fragments from the footwall are entrained in the calcite, and appear to be the result of fragmentation during faulting, which were subsequently suspended in the calcite. This relationship suggests that carbonate-rich fluids have emplaced shortly after fragmentation.

Stop 4 is near a complex boundary between the Salt Lake City and Provo segments where the main fault zone curves around the base of the Wasatch Mountains (fig. 10; Schwartz and Coppersmith, 1984; Bruhn et al., 1987; Bruhn et al., 1990). Faulting in this area may have initiated by 17 Ma based on a K-Ar date of hydrothermal sericite (Parry and Bruhn, 1986). Apatite fission track ages record onset of rapid uplift and erosion by 10 Ma, with an ongoing average vertical displacement rate from 0.5 to 0.8 mm/yr (Evans et al., 1985; Kowallis et al., 1990). Total vertical displacement is greater than 11 km (Parry and Bruhn, 1986). Within the boundary, the two main segments display several bends and a ~6 km left step along an E-striking cross fault, which continues into the footwall as the Deer Creek fault. A complexly deformed bedrock ridge lies above the subsurface projection of the boundary within the hanging wall to the southwest in the Traverse Mountains. The boundary marks a change in rupture history between the Salt Lake City and Provo segments and its subsurface projection corresponds to a region of diffuse, historic microseismic activity, including a $M_L=5$ earthquake in 1991 (Pechman, 1992), indicating that the boundary is important in nucleating and stopping ruptures at a range of scales. The fault zone cuts and deforms the Little Cottonwood granitic stock and well-exposed uplifted fault rock provides an excellent opportunity to examine the nature of deformation and fluid-rock interaction that occurred at deeper levels near the base of the seismogenic layer around the boundary.

At a megascopic scale, the segments are divided into crudely planar sections that vary systematically in orientation around the boundary (fig. 10), although in detail, fault sections display roughness at a variety of scales. Average slip directions also vary systematically around the boundary, but are locally variable along associated minor faults. The Salt Lake City segment is divided into four sections that define an approximately cylindrical bend with an axis plunging 25° toward 230° (S1–S4). Strikes of the sections vary from NE to NW, dips decrease from 45° to 25° around the bend, and trends of slip directions vary from W to WSW (fig. 11). The Deer Creek cross fault is divided into three sections (D1–D3) that dip 25° SW to 35° S and link the two main segments. Average slip directions plunge gently SW, but slip lineations on associated minor faults display large variations. Overall, slip directions diverge slightly around the bend in the Salt Lake City segment and along the Deer Creek fault, with complex deformation along minor faults in the boundary accommodating displacement transfer. WSW-striking normal faults that bound a fractured bedrock ridge in the hanging wall form a roughly conical structure parallel to and above the boundary axis, and accommodate both SW and NW extension. The northern part of the Provo segment is divided into 2 sections (P1 and P2) that dip moderately W to SW and have WSW-trending slip directions.

Observed slip directions for fault networks at different scales provide a record of "average" paleostress tensors, although in detail the stress field was spatially and temporally variable. Average slip directions for the main fault sections are consistent with a best-fit regional stress tensor having a steeply W-plunging σ_1 axis, a gently NNW-SSE-plunging σ_2 axis, a gently ENE–WSW-plunging σ_3 axis, and a stress magnitude ratio ϕ of 0.5 (fig. 11) (where $\phi = \sigma_1,-\sigma_3/\sigma_2-\sigma_3$), where $\sigma_1 > \sigma_2 > \sigma_3$ are the principal stresses. These values are similar to results obtained by Gibler (1986) for fault networks along the Salt Lake City segment. The regional σ_3 axis is subparallel to the trend of the boundary axis, but slip directions for individual faults diverge slightly around the boundary. Slip directions on minor faults within domains around the boundary display more complicated patterns. Domains away from the boundary have estimated local stress tensors similar to the regional tensor, but local stress tensors for domains within the boundary have lower values of ϕ and greater variations in

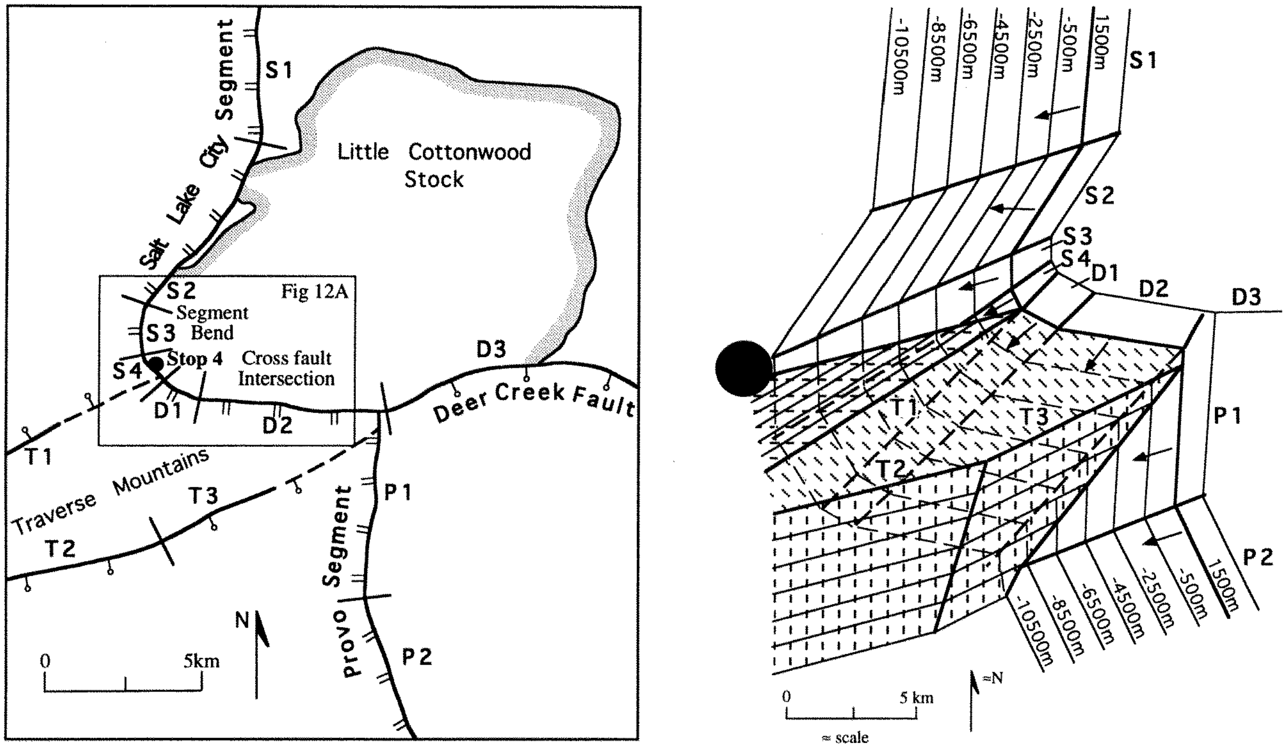

Figure 10. A. Index map of the large-scale structure of the Wasatch fault at a composite segment-bend, cross-fault-interaction boundary near stop 4. The Salt Lake and Provo segments and Deer Creek fault are divided into approximately planar fault sections labeled S1 to S4, P1 to P2, and D1 to D3. Major hanging wall faults that bound the Traverse Mountains are labeled T1 to T3. Location of figure 12A indicated.
B. Perspective view down and to NE of large-scale geometry of fault sections. Structure contours indicated and location of 1991 ML ~5 earthquake focus shown by solid circle. Average slip directions, indicated by arrows, diverge slightly around the boundary. Sections labeled same as in part A.

the trends of σ_3 axes. The decrease in ϕ for minor fault networks within the boundary may be related to divergence of slip vectors on the main fault sections around the bend, resulting in non-plane strain with components of both SW and NW extension. Also, individual minor faults in the boundary display large variations in slip directions, reflecting non-plane stsrain and temporal variations in stress, which may be partly related to complex deformation near rupture tips and intersecting fault sections.

The intensity of deformation and alteration varies with structural position within the fault zone and boundary (fig. 12; Yonkee and Bruhn, 1990; Bruhn et al., 1994). Relatively undeformed and unaltered footwall granite away from the fault, referred to as zone 0, is cut by widely spaced (average spacing > 1 m), relatively long (average trace lengths > 1 m), fractures (fig. 9). The fractures form simple networks consisting of steeply dipping and subhorizontal sets, and some fractures display limited alteration and minor extension or shear. Footwall granite grades upward into a transition zone of heterogeneously deformed and altered rock, with a preserved thickness that varies from about 20 m to > 200 m within the boundary (fig. 12b). The lower part of the transition zone, referred to as zone 1, is cut by closer spaced (dm-scale average spacing) fractures that display more intersections, mutual truncation, and offset compared to footwall granite in zone 0 (figs. 12c, 13b). The upper, more deformed part of the transition zone, referred to as zone 2, is characterized by complex, anastomosing networks of closely spaced (cm-scale average spacing) fractures and minor faults (figs. 12c, 13c). Most trace lengths are less than 1 m, reflecting continued mutual offset and truncation of fracture and faults that display numerous intersections. Widespread veins are generally steeply dipping, display evidence for repeated cracking and sealing events, and produce locally significant dilation and horizontal extension, although some veins are activated as minor faults with both reverse and normal slip. The transition zone grades upward into a slip zone (zone 3) composed of discontinuous lenses of breccia, finely comminuted cataclasite, highly altered and partly recrystallized phyllonite, and large striated slip surfaces (fig. 12c). The slip zone has a preserved thickness generally < 10 m, but its total thickness is uncertain due to

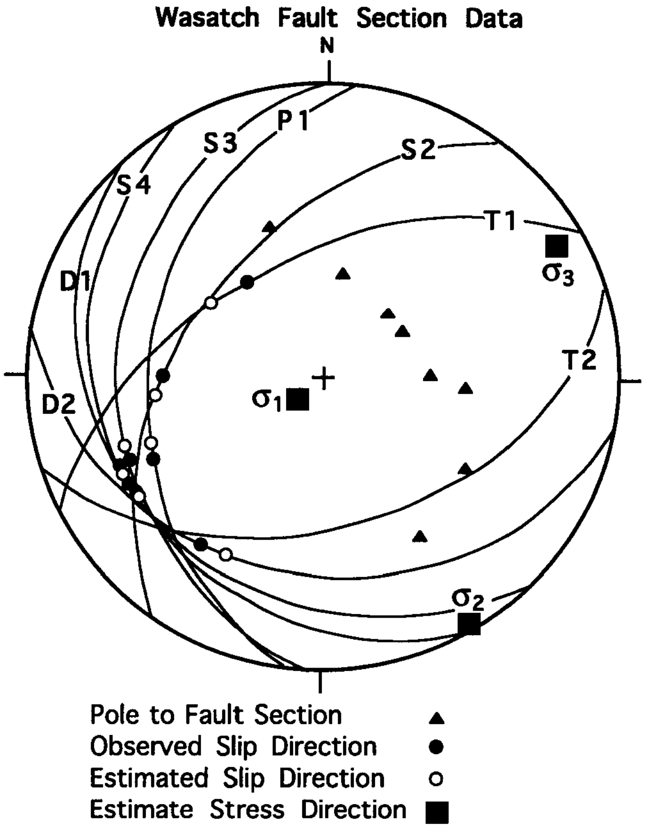

Figure 11. Equal area stereogram showing geometric relations of major structures. Average fault sections shown by great circles, poles to fault sections shown by triangles, observed average slip directions indicated by solid circles, and estimated average slip directions from stress inversion indicated by open circles. Principal stress directions estimated from stress inversion shown by squares. See figure 10A for explanation of fault section labels.

truncation by major slip surfaces. A phyllonitic fabric, defined by stretched quartz grains, fractured and boudinaged feldspar grains, and preferred orientation of altered mica aggregates is locally developed and overprinted by fractures, carbonate- and zeolite-filled veins, and cataclastic zones. Veins of partly altered and recrystallized pseudotachylyte both cross cut and are deformed by the phyllonitic fabric, recording overlapping plastic flow and brittle faulting during generation of large earthquakes (Yonkee and Bruhn, 1990). Some large slip surfaces also have associated ultracataclasite dikes that are injected into adjacent wall rock.

Changes in fracture networks are evident along our hike across the fault zone. At point 4-1 in the lower part of the transition zone (fig. 12a), the network includes: (1) a dominant set of relatively long, close-spaced, moderately W-dipping, shear fractures parallel to the main fault zone; (2) a set of shorter, variably spaced, steeply dipping, hybrid fractures that connect set 1 fractures; (3) a set of steeply dipping, hybrid and extensional cross fractures that strike at high angles to the main fault zone; and (4) other locally developed sets (fig. 12c). At point 4-2 in the middle part of the transition zone, the fracture network is broadly similar, but fracture intensity increases, additional sets are locally developed, and alteration is more widespread (fig. 13b). Some fractures, including the dominant set of shear fractures (set 1), show evidence of episodic dilation with precipitation of quartz veins during periods of high fluid pressure. Some veins were deformed during later shearing, recording repeated episodes of tensile and shear fracturing, fluid influx, and sealing. Continuing southwest in the upper part of the transition zone, the fracture network is very complex, with multiple sets of mutually offset, closely spaced fractures. The geometry of the fracture network varies over short distances within the boundary and includes synthetic normal faults and shear fractures, antithetic faults and shear fractures, steeply dipping hybrid fractures and veins that are locally activated as faults, cross fractures with varying slip directions, other local fracture sets, and random, curviplanar fractures (fig. 13e). Different slip directions on fractures and faults of varying orientation and the sinuous nature of many faults results in mutual offset and interlocking, and may lead to geometric hardening.

At point 4-3 in the slip zone, cataclasite and phyllonite are intensely deformed and altered, and locally cut by large slip surfaces, although most mesoscopic fractures are difficult to trace due to truncation, healing and sealing, and pervasive microcracking. Rare, variably deformed pseudotachylyte veins occur within both cataclasite and phyllonite.

Hydrothermal alteration in the transition zone is concentrated along fracture, vein, and microcrack networks, and alteration is widespread in the slip zone, especially in phyllonite. Two main alteration assemblages are present:

Figure 12. A. Generalized geologic map of area around stop 4. Route of hike and sites indicated. Units are: zone 0–undeformed granitic rock of footwall; zone 1–lower, less deformed part of transition zone; zone 2–upper, more deformed part of transition zone; zone 3–slip zone of highly deformed phyllonite and cataclasite; Q–undivided Quaternary deposits; Pz-Cz–undivided Paleozoic to Cenozoic rocks in hanging wall.
B. Cross sections A-A′ and B-B′ illustrating variations in thickness of fault zones within the boundary. Sectiop B-B′ within the middle part of the boundary has a thick, complexly deformed zone 2 interval. See part A for locations of section lines.
C. Schematic block diagrams A-A′ and B-B′ illustrating styles of fracture networks within the boundary. Veins indicated by stippled pattern, phyllonite by short wiggly lines, and cataclasite by short dashed lines.

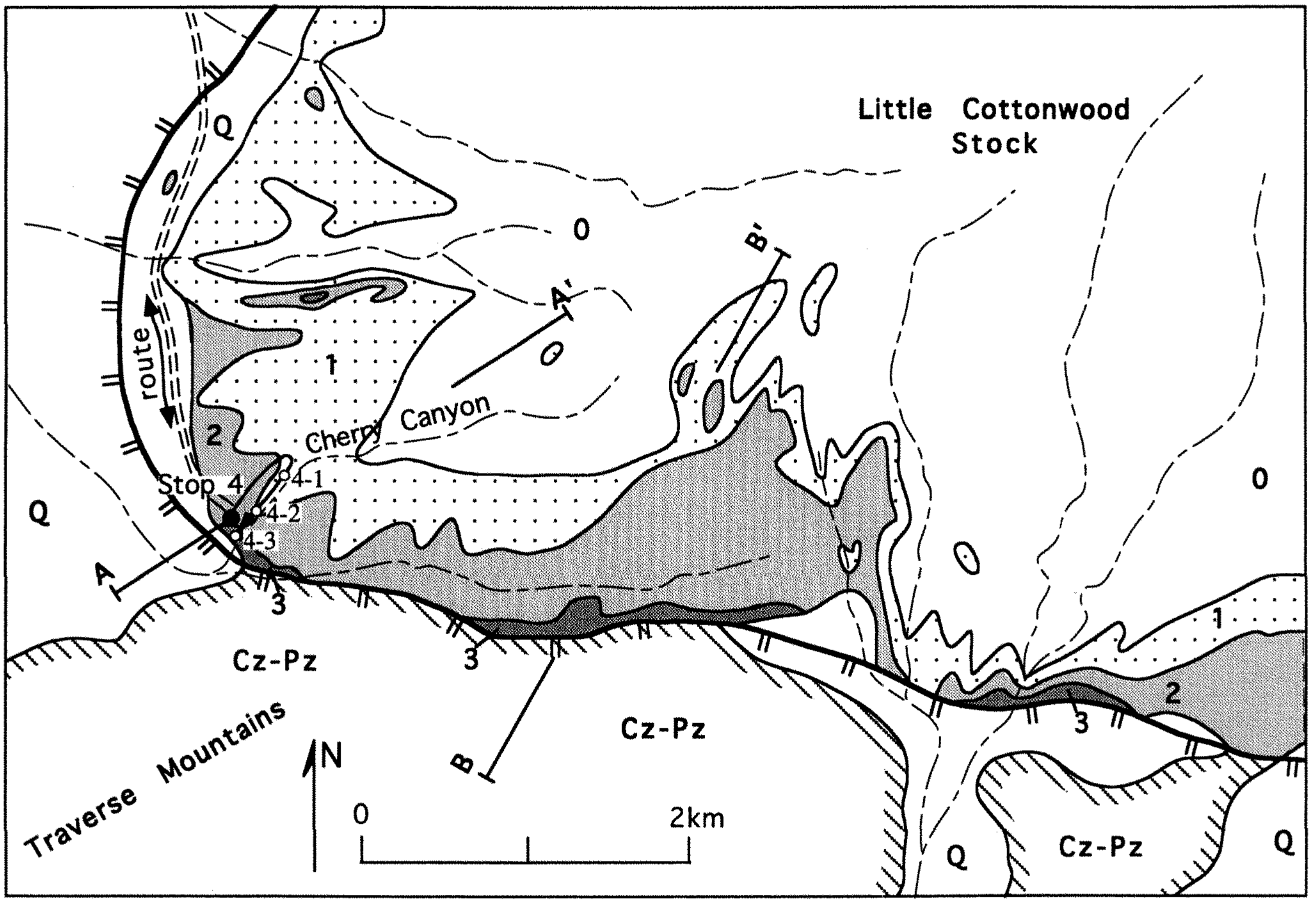
Little Cottonwood
Stock
Q
0
B'
A'
1
route
2
Cherry Canyon
Stop 4
4-1
4-2
4-3
A
3
Cz-Pz
Traverse Mountains
N
B
0
2km
1
2
3
Q

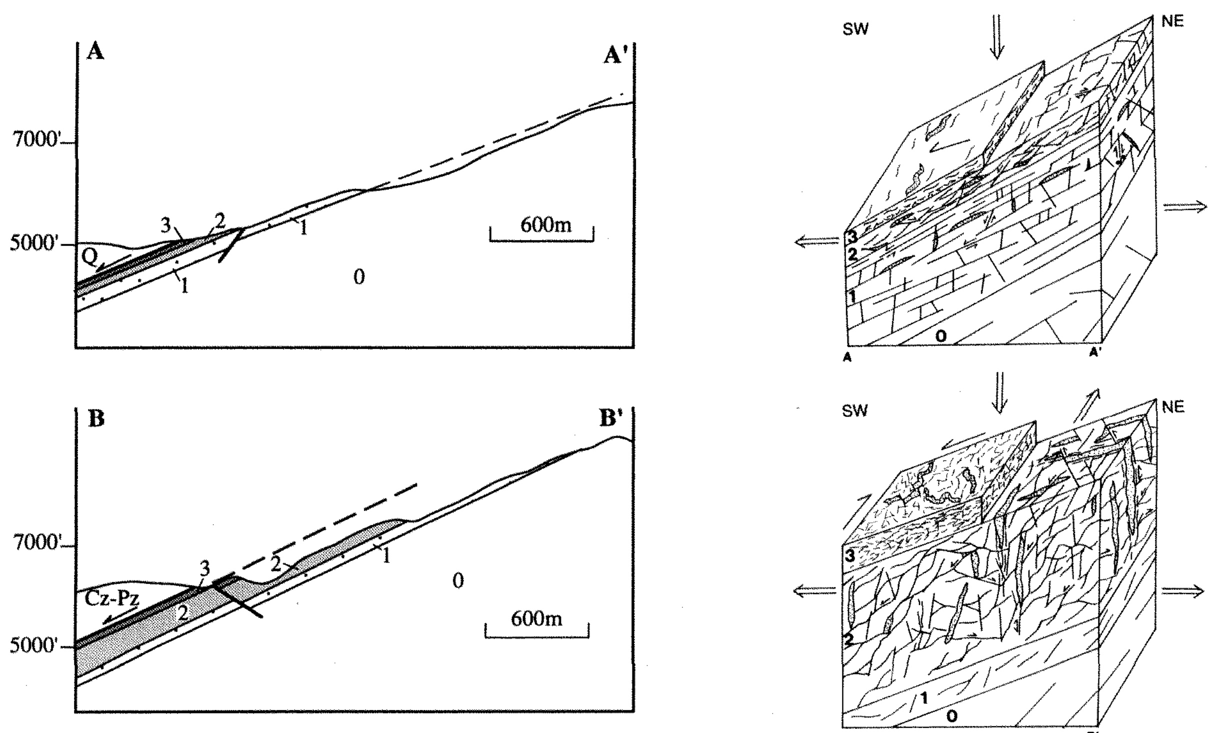
A
A'
7000'
5000'
3
2
1
Q
0
600m
B
B'
Cz-Pz
600m
SW
NE
3
2
1
0
A
A'
SW
NE
3
2
1
0
B
B'

abilities related to fractures are greater in the transition zone compared to the footwall granite and range from on the order of 10^{-12} to 10^{-14} m^2 at high fluid pressures to 10^{-16} to 10^{-18} m^2 at low fluid pressures, reflecting a non-linear dependance of aperture on effective normal stress (Bruhn et al., 1994). In detail, permeability is anisotropic, and estimated permeability tensors in the transition zone have long axes at low angles to the main fault zone. Sealing and healing episodically closed fractures such that actual permeabilities may have been lower, particularly during inter-seismic periods. Permeability of the slip zone is uncertain. Estimated elastic moduli related to fractures decrease from the footwall into the transition zone, and are between 10 and 40% of intact rock. Elastic moduli are difficult to estimate within the slip zone due to pervasive fracturing and micro-cracking. Note that reduced moduli also result in reduced seismic velocities in the fault zone.

This ends the trip. Retrace the route to 12,300 South, return to I-15, and the Salt Palace. Thank you.

REFERENCES CITED

Allmendinger, R.W., Marrett, R A , and Cladouhos, T., 1992, Faultkin, a Program for analyzing fault slip data for the Macintosh computer. Copyrighted software.

Arabasz, W.J., and Julander, D.R., 1986, Geometry of seismically active faults and crustal deformation within the Basin and Range-Colorado Plateau transition, *in* Mayer, L., ed., Extensional tectonics of the south-western United States. A perspective on processes and kinematics, Geological Society of America Special Paper 208, p. 43–74.

Arabasz, W.J., Pechmann, J.C., and Brown, E.D , 1992, Observational seismology and the evaluation of earthquake hazards and risk in the Wasatch Front area, Utah, *in* Gori, P.L., and Hays, WW, eds., Assessment of regional earthquake hazards and risk along the Wasatch Front, Utah. U.S. Geological Survey Professional Paper 1500-D, 36 pp.

Arabasz, W.J., Smith, R.B., and Richins, WD., 1978, Earthquake studies along the Wasatch front, Utah. Network monitoring, seismicity, and seismic hazards, *in* Arabasz, W.J., Smith, R.B., and Richins, W.D., eds , Earthquake studies in Utah, 1850–1978, p. 253–285.

Baker, A A., 1964, Geology of the Orem quadrangle, Utah, U.S. Geological Survey Map GQ-241.

Bruhn, R.L., Gibler, P.R., and Parry, W.T., 1987, Rupture characteristics of normal faults: an example from the Wasatch fault zone, Utah, *in* Coward, M.P., Dewey, J F., and Hancock, P.L., eds., Continental Extensional Tectonics. Geological Society of London Special Publication 28, p. 337–353.

Bruhn, R.L , Gibler, P.R., Houghton, W., and Parry, W.T., 1992, Structure of the Salt Lake segment, Wasatch normal fault zone. Implications for rupture propagation during normal faulting, *in* Gori, P.L., and Hays, W.W., eds., Assessment of regional earthquake hazards and risk along the Wasatch Front, Utah· U.S. Geological Survey Professional Paper 1500-H, 25 p.

Bruhn, R.L., Lee, J.-J., and Yonkee, W.A., 1990a, Structural properties of the American Fork, Provo, and part of the Spanish Fork subsegments, Wasatch normal fault zone, Utah. Utah Geological Survey Open-File Report 186, 43 pp

Bruhn, R.L., Yonkee, W.A., and Parry, WT, 1990b, Structural and fluid-chemical properties of seismogenic normal faults: Tectonophysics, v. 175, p. 139–157.

Bruhn, R.L., Parry, W.T., Yonkee, W.A., and Thompson, T., 1994, Fracturing and hydrothermal alteration in normal fault zones. Pure and Applied Geophysics, v. 142, p. 609–643.

Bryant, B., 1984, Reconnaissance geologic map of the Precambrian Farmington Canyon complex and the surrounding rocks in the Wasatch Mountains between Ogden and Bountiful, Utah. U.S. Geological Survey Miscellaneous Investigations Series Map I-1447, scale 1.50,000.

Bryant, B., 1988, Geology of the Farmington Canyon Complex, Wasatch Mountains, Utah: U.S. Geological Survey Professional Paper 1476, 54 p.

Bryant, B., 1990, Geologic map of the Salt Lake City 30′ x 60′ quadrangle, north-central Utah, and Uinta County, Wyoming: U S Geological Survey Miscellaneous Investigations Map I-1944, scale 1·100,000.

Bryant, B., Naeser, C.W., Marvin, R.F., and Mehnert, H.H., 1989, Ages of Late Paleogene and Neogene tuffs and the beginning of rapid regional extension, eastern boundary of the Basin and Range Province near Salt Lake City, Utah: U.S. Geological Survey Bulletin 1787, 37 p.

Buss, W.R., and Peterson, D., 1964, The Wasatch Fault in Weber and Davis Counties, Utah, *in* Marsell, R.E., ed., The Wasatch Fault zone in north central Utah, Guidebook to the Geology of Utah #18, Utah Geological Survey, p. 51–52.

Cowie, P.A., and Scholz, C.H., 1992, Growth of the faults by accumulation of seismic slip. Journal of Geophysical Research, v. 97, p. 11,085–11,095.

Crittenden, M.D., Jr., 1965a, Geology of the Draper quadrangle, Utah. U.S. Geological Survey Map GQ-377, scale 1:24,000.

Crittenden, M D., Jr, 1965b, Geologic map of the Sugar House quadrangle: U.S. Geological Survey Map GQ-380, scale 1.24,000.

Crittenden, M.D., Jr., and Sorensen, M.L., 1985a, Geologic map of the Mantua quadrangle and part of the Willard quadrangle, Box Elder, Weber, and Cache Counties, Utah. U.S. Geological Survey Map I-1605, scale 1:24,000.

Crittenden, M.D., Jr., and Sorensen, M L., 1985b, Geologic map of the North Ogden quadrangle and part of the Ogden and Plain City quadrangles, Box Elder and Weber Counties, Utah. U.S. Geological Survey Map I-1606, scale 1.24,000.

Davis, F.D., 1983, Geologic map of the central Wasatch Front, Utah. Utah Geological and Mineral Survey Map 54-A, scale 1·100,000.

Davis, F.D., 1985, Geology of the northern Wasatch front: Utah Geological and Mineral Survey Map 53-A, 2 sheets, scale 1 100,000.

Eardley, A.J., 1939, Structure of the Wasatch-Great Basin region: Geological Society of America Bulletin, v. 50, p. 1277–1310

Eardley, A.J., 1944, Geology of the north-central Wasatch mountains, Utah: Bulletin of Geological Society of America, v. 55, p. 819–894.

Eardley, A.J., and Hatch, R.A., 1940, Precambrian crystalline rocks of north-central Utah. Journal of Geology, v. 48, p. 58–72.

Evans, J.P., and Langrock, H , 1994, Structural analysis of the Brigham City-Weber Segment boundary zone, Wasatch normal fault, Utah: Implications for fault growth and structure: Pure and Applied Geophysics, v. 142, p. 663–684.

Evans, S.H., Parry, W.T., and Bruhn, R.L., 1985, Thermal, mechanical, and chemical history of Wasatch fault cataclasite and phyllonite, Traverse Mountains area, Salt Lake City, Utah. From K/Ar and fission track measurements U S Geological Survey Open-File Report 86-31, p. 410–415.

Gephart, J.W., 1990a, Stress and the direction of slip on faults: Tectonics, v. 9, p. 845–858.

Gephart, J.W., 1990b, FMSI A fortran program for inverting fault/slickenside and earthquake focal mechanism data to obtain the regional stress tensor: Computers and Geosciences, v. 16, p 953–989.

Gilbert, G.K., 1890, Lake Bonneville: U.S. Geological Survey Monograph 1, 438 p.

Gilbert, G K , 1928, Studies of Basin-Range structure: U.S. Geological Survey Professional Paper 153, 89 p

Grocott, J., 1981, Fracture geometry of pseudotachylyte generation. A study of shear fractures formed durıng seismic events. Journal of Structural Geology, v. 3, p. 169–178.

Hecker, S , 1993, Quaternary tectonics of Utah with emphasıs on earthquake-hazard characterization. Utah Geological Survey Bulletın, v. 127, 157 pp

Hıntze, L.F., 1980, Geologic map of Utah Utah Geological and Mineral Survey Map A-2, scale 1.500,000.

Kowallıs, B.J., Ferguson, J., and Jorgensen, G.J., 1990, Uplift along the Salt Lake segment of the Wasatch Fault from apatıte and zircon fission track datıng ın the Little Cottonwood Stock, *in* Durranı, S.A., and Benton, E.V., eds., Proceedings of the 6th International Fıssıon Track Dating Workshop, Nuclear Tracks and Radiation Measurements 17, Pergamon, Oxford, p. 325–329.

Lınk, P.K., Crook, S.R., and Chidsey, T.C., Jr., 1985, Hinterland structure, paleozoic stratigraphy and duplexes of the Wıllard thrust system, Bannock, Wellsville and Wasatch ranges, southeastern Idaho and northern Utah, *in* Kerns, G.L., and Kerns, R.L., Jr., eds., Orogenic Patterns and Stratigraphy of North-Central Utah and Southeastern Idaho, Utah Geological Associatıon Publication 14, p. 314–328.

Link, P.K., and Smith, C.H., 1992, Late Proterozoic and Early Cambrian stratigraphy, paleobiology, and tectonics: Northern Utah and southeastern Idaho, *in* Wilson, J.R., eds., Field Guide to Geologıc Excursions in Utah and Adjacent Areas of Nevada, Idaho, and Wyoming, Utah Geological Survey Miscellaneous Publıcation 92-3, p 461–481.

Mabey, D.R., 1992, Subsurface geology along the Wasatch Fault area, Utah, *in* Gori, P.L., and Hays, W.W., eds., Assessment of regional earthquake hazards and rısks along the Wasatch Front, Utah· U.S. Geologıcal Survey Professıonal Paper 1500-C, 16 p.

Machette, M.N., 1988, In the footsteps of G.K. Gilbert—Lake Bonnevılle and *neotectonics of the eastern Basin and Range Province.* Utah Geologıcal and Mineral Survey Mıscellaneous Publication 88-1, 120 pp

Machette, M.N., 1992, Surficial geologic map along the Wasatch fault zone in the eastern part of the Utah Valley, Utah County, and parts of Salt Lake and Juab Countıes, Utah U.S. Geologıcal Survey Miscellaneous Investigatıons Series Map I-2095, scale 1:50,000.

Machette, M.N., Personius, S.F., Nelson, A.R., Schwartz, D.P., and Lund, W.R., 1991, The Wasatch fault zone, Utah. Segmentatıon and history of Holocene earthquakes. Journal of Structural Geology, v. 13, p. 137–149.

Machette, M N., Personius, S.F., Nelson, A.R., Schwartz, D.P, and Lund, W.R , 1989, Segmentatıon models and Holocene movement history of the Wasatch fault zone, Utah, *in* Schwartz, D.P., and Sibson, R.H., eds , Proceedings of Conference XLV—Fault segmentation and controls on rupture initiation and termınation: U.S Geologıcal Survey Open-File Report 89-315, p. 229–245.

Machette, M.N., Personius, S F., and Nelson, A.R., 1992, Paleoseismology of the Wasatch fault zone—A summary of recent ınvestigations, conclusıons, and interpretations, *in* Gorı, PL , and Hays, W.W., eds., Assessıng regıonal earthquake hazards and risk along the Wasatch Front, Utah. U.S. Geological Survey Professional Paper 1500-A, p. A1–A71.

Marsell, R.E., 1964, The Wasatch Fault in Salt Lake County, Utah, *in* Marsell, R.E., ed., The Wasatch Fault zone in north central Utah, Guıdebook to the Geology of Utah #18, Utah Geological Survey, p. 31–50.

Marsell, R E., 1969, The Wasatch Fault zone ın north central Utah, *in* Guidebook of northern Utah, Utah Geological and Mineralogical Survey Bulletin 82, p. 124–129.

McCalpın, J.P., and Nishenko, S.P., 1996, Holocene paleoseismicity, temporal clustering, and probabilıtıes of future large (M >7) earthquakes on the Wasatch fault zone, Utah. Journal of Geophysıcal Research, v. 101, p. 6233–6253.

Naeser, C.W., Bryant, B., Crittenden, M.D., Jr., and Sorensen, M.L., 1983, Fission-track ages of apatıte in the Wasatch Mountains, Utah. an uplift study, *in* Miller, D.M., Todd, V.R., and Howard, K.A., eds., Tectonic and stratıgraphıc studies in the eastern Great Basın. Geologıcal Socıety of America Memoir 157, p. 29–36.

Nelson, A R , 1988, The northern part of the Weber segment of the Wasatch fault zone near Ogden, Utah, *in* Machette, M.N , ed., In the Footsteps of G.K. Gilbert—Lake Bonnevılle and Neotectonıcs of the Eastern Basin and Range Province Utah Geologıcal and Mıneral Survey Miscellaneous Publication 88-1, p 33–37.

Nelson, A.R., and Personius, S.F., 1993, Surficıal geologic map of the Weber segment, Wasatch fault zone, Weber and Davıs Counties, Utah U.S Geological Survey Map I-2199, scale 1:50,000

Oda, M., Hatsuyama, Y., and Ohnıshı, Y., 1987, Numerical experiments on permeabılity tensor and its application to jointed granıte at the Stripa Mine, Sweden. Journal of Geophysical Research, v. 92, p 8037–8048

Oda, M., 1986, An equivalent continuum model for coupled stress and fluid flow analysis in jointed rock masses Water Resources Research, v. 22, p. 1845–1856.

O'Connell, R.J., and Budiansky, B., 1974, Seismic velocities ın saturated and dry cracked solids. Journal of Geophysical Research, v 79, p 5412–5426

Pack, FJ , 1926, New discoveries relatıng to the Wasatch fault Amerıcan Journal of Science, v. 27, p. 399–410.

Parry, W.T., and Bruhn, R.L., 1986, Pore fluid and seismogenıc characterıstıcs of fault rock at depth on the Wasatch fault, Utah. Journal of Geophysical Research, v. 91, p. 730–744.

Parry, W.T, and Bruhn, R.L., 1987, Fluid ınclusıon evıdence for mınımum 11 km vertıcal offset on the Wasatch fault, Utah. Geology, v. 15, p. 67–70.

Parry, W.T., and Bruhn, R.L., 1990, Fluid pressure transients on seismogenic normal faults. Tectonophysıcs, v. 179, p. 335–344.

Parry, WT, Wılson, P.N., and Bruhn, R.L., 1988, *Pore fluid chemistry* and chemıcal reactions on the Wasatch normal fault, Utah Geochemıca et Cosmochımıca Acta, v. 52, p. 2053–2063.

Pashley, E.F., Jr., and Wiggins, R A., 1972, Landslıdes of the northern Wasatch Front, *in* Environmental geology of the Wasatch Front, 1971. Salt Lake City, Utah, Utah Geologıcal Assocıatıon Publication 1, p. K1–K16.

Pavlıs, T.L., Serpa, L.F, and Keener, C , 1993, Roles of seismogenic processes ın fault-rock development, an example from Death Valley, California. Geology, v. 21, p. 267–270.

Pavlıs, T.L., and Smıth, R.B , 1980, Slip vectors from faults near Salt Lake City from Quaternary displacement and seismicıty, *in* Arabasz, WJ , Smıth, R.B., and Rıchıns, W.D., eds., Earthquake Studies in Utah: Salt Lake Cıty, Utah, Unıversıty of Utah, p. 378–382.

Pechmann, J.C., 1992, Focal mechanısm and seismotectonıc settıng, *in* The March 16, 1992 M 4.2 Western Traverse Mountaıns Earthquake, Salt Lake County, Utah Utah Geological Survey, Open-File Report 255, p 3–7.

Personius, S.F., 1990, Surficıal geologıc map of the Brıgham Cıty segment and adjacent parts of the Weber and Collınston segments, Wasatch fault zone, Box Elder and Weber Countıes, Utah. U.S. Geologıcal Survey Map I-1979, scale 1.50,000.

Personıus, S.F., and Scott, W.E , 1992, Surficial geologic map of the Salt Lake Cıty segment and parts of adjacent segments of the Wasatch fault zone, Davıs, Salt Lake, and Utah Counties, Utah: U.S Geological Survey Miscellaneous Investigations Series Map I-2106, scale 1 50,000

Petit, J.P., 1987, Criterıa for the sense of movement on fault surfaces ın brittle rocks: Journal of Structural Geology, v 9, p 597–608

Power, W.L., and Tullis, T.E , 1992, The contact between opposıng fault surfaces at Dıxıe Valley, Nevada, and ımplıcatıons for fault mechanıcs Journal of Geophysical Research, v. 97, p. 15425–15435.

Royse, F., Warner, M A , and Reese, D L , 1975, Thrust belt structural geometry and related stratıgraphıc problems, Wyomıng-Idaho-northern

Utah, *in* Boyland, D.W., ed., Deep drilling frontiers of the central Rocky Mountains: Rocky Mountain Association of Geologists, p. 41–54.

Schirmer, T.W., 1988, Structural analysis using thrust fault hanging-wall sequence diagrams: Ogden duplex, Wasatch Range, Utah: American Association of Petroleum Geologists Bulletin, v. 72, p. 573–585.

Scholz, C.H., 1990, The mechanics of earthquakes and faulting: Cambridge University Press, 439 pp.

Schwartz, D.P., and Coppersmith, K.J., 1984, Fault behavior and characteristic earthquakes—Example from the Wasatch and San Andreas fault zones: Journal of Geophysical Research, v. 89, p. 5681–5698.

Scott, W.E., 1988, G.K. Gilbert's observations of post-Bonneville movement along the Warm Springs Fault, Salt Lake City, Utah, *in* Machette, C., ed., In the footsteps of G.K. Gilbert—Lake Bonneville and neotectonics of the eastern Basin and Range Province: Utah Geological and Mineral Survey Miscellaneous Publication 88-1, p. 44–46.

Smith, R.B., and Bruhn, R.L., 1984, Intraplate extensional tectonics of the eastern Basin-Range: Inferences on structural style from seismic reflection data, regional geophysics and thermal-mechanical models of brittle-ductile deformation: Journal of Geophysical Research, v. 87, p. 5733–5762.

Swan, F.H., III, Schwartz, D.P., and Cluff, L.S., 1980, Recurrence of moderate to large magnitude earthquakes produced by surface faulting on the Wasatch fault zone, Utah: Bulletin of the Seismological Society of America, v. 70, p. 1431–1462.

Van Horn, R., 1982, Surficial geologic map of the Salt Lake City North quadrangle, Davis and Salt Lake Counties, Utah: U.S. Geological Survey Miscellaneous Investigations Map I-1404, scale 1:24,000.

Van Horn, R., and Crittenden, M.D., Jr., 1988, Map showing surficial units and bedrock geology of the Fort Douglas quadrangle and parts of the Mountain Dell and Salt Lake City North quadrangles, Davis, Salt Lake, and Morgan Counties, Utah. U.S. Geological Survey Miscellaneous Investigations Map I-1762, scale 1.24,000.

Wheeler, R.L., and Krystinik, K.B., 1992, Persistent and nonpersistent segmentation of the Wasatch fault zone, Utah: Statistical analysis for evaluation of seismic hazard: U.S. Geological Survey Professional Paper 1500-B.

Yonkee, W.A., 1992, Basement-cover relations, Sevier orogenic belt, northern Utah: Geological Society of America Bulletin, v. 104, p. 280–302.

Yonkee, W.A., and Bruhn, R.L., 1990, Geometry and mechanics of a structural boundary, Wasatch fault zone, Utah, *in* Bruhn, R.L., Lee, J., and Yonkee, W.A., eds., Structural properties of the American Fork, Provo, and Spanish Fork subsegments, Wasatch normal fault zone, Utah: Utah Geological and Mineral Survey Open-File Report 186, 50 p.

Yonkee, W.A., Evans, J.P., and DeCelles, P.G., 1992, Mesozoic tectonics of the northern Wasatch Range, Utah, *in* Wilson, J.R., ed., Field guide to geologic excursions in Utah and adjacent areas of Nevada, Idaho, and Wyoming: Utah Geological Survey Miscellaneous Publication 92-3, p. 429–460.

Zoback, M.L., 1983, Structure and Cenozoic tectonism along the Wasatch fault zone, *in* Miller, D.M., Todd, V.R., and Howard K.A., eds., Tectonic and stratigraphic studies in the eastern Great Basin: Geological Society of America Memoir 157, p. 3–27.